CMST 17(1) 17-23 (2011)

DOI:10.12921/cmst.2011.17.01.17-23

COMPUTATIONAL METHODS IN SCIENCE AND TECHNOLOGY **17(1-2)**, 17-23 (2011)

Phase Diagram of Diblock Copolymer Melt in Dimension $d = 5$

M. Dzięcielski, K. Lewandowski, M. Banaszak

Faculty of Physics, A. Mickiewicz University
ul. Umultowska 85, 61-614 Poznań, Poland
e-mail: mbanasz@amu.edu.pl

(Received: 21 November 2011; revised: 05 December 2011; accepted: 09 December 2011; published on-line: 15 December 2011)

Abstract: Using the self-consistent field theory (SCFT) in spherical unit cells of various dimensionalities, D, a phase diagram of a diblock, A-b-B, is calculated in 5 dimensional space, $d = 5$. This is an extension of a previuos work for $d = 4$. The phase diagram is parameterized by the chain composition, f, and incompatibility between A and B, quantified by the product χN. We predict 5 stable nanophases: layers, cylinders, 3D spherical cells, 4D spherical cells, and 5D spherical cells. In the strong segregation limit, that is for large χN, the order-order transition compositions are determined by the strong segregation theory (SST) in its simplest form. While the predictions of the SST theory are close to the corresponding SCFT extrapolations for $d = 4$, the extrapolations for $d = 5$ significantly differ from them. We find that the S_5 nanophase is stable in a narrow strip between the ordered S_4 nanophase and the disordered phase. The calculated order-disorder transition lines depend weakly on d, as expected

Key words: diblock copolymer melt, phase diagram, order-disorder transition, order-order transition, field theory

I. INTRODUCTION

Diblock copolymer (DBC), A-b-B, melts consist of 2 types of segments, A and B, arranged in 2 corresponding blocks. Those melts can self-assemble in 3d into various spatially-ordered nanophases, such as layers, (L), hexagonally packed cylinders, (C), gyroid nanostructures, (G), with the $Ia\bar{3}d$ symmetry, and cubically packed (either body-centered or closely packed) spherical cells (S), depending on the chain composition, f (f is the fraction of A-segments; $1 - f$ is the fraction of B-segments), degree of polymerization (number of segments), N, and the temperature-related χ parameter [1, 2]. Recently, an additional O^{70}-phase has been reported [3, 4], but it is stable in a very small region of the phase diagram. Those nanophases can be transformed into a disordered phase, for example, upon heating. It is of great interest to determine a phase diagram of such melts exhibiting order-disorder transition (ODT) lines, also referred to as binodals of microphase separation transition (MST), and order-order transition (OOT) lines. This task has been largely achieved for 3-dimensional (bulk) diblock melts by accumulating results from numerous experimental and theoretical studies [5-12], also for 2d diblock copolymer melts [13].

The L, C, and S nanophases are known as classical, whereas G and O^{70} nanophases are referred to as non-classical, or sometimes complex. The Wigner-Seitz cell of a classical phase can be approximated by D-dimensional sphere, S_D, both in the real $\vec{r}$-space and the reciprocal $\vec{k}$-space. Within this approximation, known as Unit Cell Approximation (UCA), the L, C, S nanophases correspond to S_1, S_2, and S_3, respectively, and the spacial distribution of chain segments can be mapped with a single radial variable, r, as shown in Table 1. The classical phases can be

Table 1. Unit cell equations of D-dimensionality; equations are supplemented with the unconstrained variables for corresponding d's (2, 3, 4 and 5)

	Nanophase	Cell equation	$d = 2$	$d = 3$	$d = 4$	$d = 5$	Radial coordinate
1	L (S_1)	$x^2 < R^2$	y	y, z	y, z, t	y, z, t, v	$r = \lvert x \rvert$
2	C (S_2)	$x^2 + y^2 < R^2$	*	z	z, t	z, t, v	$r = \sqrt{x^2 + y^2}$
3	S_3	$x^2 + y^2 + z^2 < R^2$	imp	*	t	t, v	$r = \sqrt{x^2 + y^2 + z^2}$
4	S_4	$x^2 + y^2 + z^2 + t^2 < R^2$	imp	imp	*	v	$r = \sqrt{x^2 + y^2 + z^2 + t^2}$
5	S_5	$x^2 + y^2 + z^2 + t^2 + v^2 < R^2$	imp	imp	imp	*	$r = \sqrt{x^2 + y^2 + z^2 + t^2 + v^2}$

*indicates the absence of unconstrained variables; imp indicates that the nanophase for this d is impossible

easily generalized to higher dimensions, in particular for $d = 5$ we can have 5 nanophases S_D, with dimensionality, D, ranging from 1 to 5.

It is interesting that a mean-field (MF) theory applied to copolymer melts [8, 14, 15], known as the Self-Consistent Field Theory (SCFT), is successful in predicting diblock phase diagrams resembling the experimental ones, as shown, for example, in Ref. [16]. The SCFT approach is based on the assumption that coarse-grained polymer chains in dense melts are Gaussian (Flory's theorem [17]), and on the MF approximation which selects the dominant contribution in the appropriate partition function, thus neglecting fluctuations.

Because, in the MF theories, it is sufficient to know the composition, f, and the product χN in order to foresee the nanophase [5, 15, 18], the diblock phase diagram can be mapped in (f, χN)-plane. The MF theories exist in many variations, both in real space ($\vec{r}$-space) [6, 7, 9] and Fourier space ($\vec{k}$-space) [2, 8].

In addition, we intend to compare the phase boundaries calculated by the SCFT (and extrapolated to the strong segregation limit) with the strong segregation theory (SST) for diblock melts, developed by Semenov [19], in which the free energy of the nanophase has three contributions, the interfacial tension and the stretching (of entropic origin) energies of the A and B blocks. These energies can be approximated by simple expressions, allowing the calculation of the OOT compositions in the SST. The main goal of this paper is to construct a phase diagram of a copolymer melt for $d = 5$, applying the SCFT method with the UCA in r-space, as presented in [6-8]. Specifically, we intend to determine the area in (f, χN)-space, in which the S_5 phase is stable, by varying both the radius, R, of the unit cell and the dimensionality, D.

In previous work [20] we calculated the phase diagram of the diblock copolymer melt for $d = 4$, and managed to answer the following questions:

1. is the S_4 nanophase stable?
2. what is the sequence of nanophases upon changing f?
3. are the binodals (ODT lines) shifted as we vary d from 1 to 4?
4. what are the strong segregation limits of the OOT lines for $d = 4$?

The answers were as follows:

1. the nanophase S_4 is stable within a relatively narrow strip between the S_3 nanophase and the disordered phase,
2. the sequence of nanophases appropriate for the UCA in $3d$ is preserved, starting from $f = 1/2$, L, C, S_3, and there is an additional S_4 nanophase in $4d$,
3. the ODT binodals depend weakly on d, and they are shifted as d is varied,
4. the SST compositions, $f_{L/C}$, f_{C/S_3}, and f_{S_3/S_4} are close to the corresponding extrapolations from the self-consistent field theory.

In this work, as in Ref. 20, the following questions are posed:

1. is the S_5 nanophase stable?
2. what is the position of the S_5 nanophase in sequence of phases upon changing f?
3. are the binodals (ODT lines) shifted as we vary d from 4 to 5?
4. what are the strong segregation limits of the OOT lines for $d = 5$?

II. METHOD

The incompressible copolymer melt is modeled as a collection of n diblock chains confined in volume V. Each

chain, labeled $\alpha = 1, 2, ..., n$, can take any Gaussian configuration (in accordance with the Flory's Theorem [17]) parameterized from $s = 0$ to $s = f$ for A-segments, and from $s = f$ to $s = 1$ for B-segments. Up to a multiplicative constant, the partition function for a single Gaussian chain in external fields $W_A(\mathbf{r})$ and $W_B(\mathbf{r})$ acting on segments A and B, respectively, is

$$\mathcal{Q}[W_A, W_B] \equiv \int \widetilde{\mathcal{D}}\mathbf{r}_\alpha(\cdot) \times \times \exp\left[-\int_0^f ds W_A(\mathbf{r}_\alpha(s)) - \int_f^1 ds W_B(\mathbf{r}_\alpha(s))\right] \quad (1)$$

The path integral, $\int \widetilde{\mathcal{D}}\mathbf{r}_\alpha(\cdot)$, is taken over single-chain trajectories, $\mathbf{r}_\alpha(s)$, with Wiener measure expressed as $\widetilde{\mathcal{D}}\mathbf{r}_\alpha = \mathcal{D}\mathbf{r}_\alpha P[\mathbf{r}_\alpha; 0, 1]$, and

$$P[\mathbf{r}_\alpha; s_1, s_2] \propto \exp\left[-\frac{3}{2Na^2}\int_{s_1}^{s_2} ds \left|\frac{d}{ds}\mathbf{r}_\alpha(s)\right|^2\right] \quad (2)$$

Note that a is the segment size, and Na^2 is the mean squared end-to-end distance of a Gaussian chain. By Kac-Feynman theorem, Eq. 1 can be related to a Fokker-Planck partial differential equation [2], known also as a modified diffusion equation (MDE) and shown with appropriate details below (Eqs. 15 and 16).

Segments A and B interact via the χ parameter which provides an effective measure of incompatibility between them [17]. Evaluation of the full partition function of n interacting diblock chains, shown below (Eq. 3), is a highly challenging task, involving many-body interactions, both intermolecular and intramolecular.

$$Z = \int \prod_{\alpha=1}^{n} \widetilde{\mathcal{D}}\mathbf{r}_\alpha \, \delta[1 - \hat{\phi}_A - \hat{\phi}_B] \exp\left[-\chi\rho_0 \hat{\phi}_A \hat{\phi}_B\right] \quad (3)$$

where δ-function enforces incompressibility (the melt is assumed to be incompressible), and

$$\hat{\phi}_A(\mathbf{r}) = \frac{N}{\rho_0}\sum_{\alpha=1}^{n}\int_0^f ds \, \delta(\mathbf{r} - \mathbf{r}_\alpha(s)) \quad (4)$$

$$\hat{\phi}_B(\mathbf{r}) = \frac{N}{\rho_0}\sum_{\alpha=1}^{n}\int_f^1 ds \, \delta(\mathbf{r} - \mathbf{r}_\alpha(s)) \quad (5)$$

are the microscopic segments densities of A and B, respectively; $\rho_0 = nN/V$ is the segment number density. After replacing microscopic segment (or particle) densities with a variety of fields [2, 6-8], by inserting and spectrally decomposing the appropriate δ-functionals, the partition function of an incompressible diblock melt is

$$Z = \mathcal{N}\int \mathcal{D}\phi_A(\cdot)\,\mathcal{D}W_A(\cdot)\,\mathcal{D}\phi_B(\cdot)\,\mathcal{D}W_B(\cdot)\,\mathcal{D}\Psi(\cdot) \times \times \exp\left[-\frac{F[\phi_A, W_A, \phi_B, W_B, \Psi]}{k_B T}\right] \quad (6)$$

where $\mathcal{N}$ is a normalization factor. The functional integral is taken over the relevant fields $\phi_A(\mathbf{r})$, $W_A(\mathbf{r})$, $\phi_B(\mathbf{r})$, $W_B(\mathbf{r})$, and $\Psi(\mathbf{r})$, with the free energy functional, $F[\phi_A, W_A, \phi_B, W_B, \Psi]$, including the single chain partition function (in external fields $W_A(\mathbf{r})$ and $W_B(\mathbf{r})$), as shown below

$$\frac{F[\phi_A, W_A, \phi_B, W_B, \Psi]}{nk_B T} \equiv -\ln\frac{\mathcal{Q}}{V} + V^{-1}\int d\mathbf{r}\big[N\chi\phi_A(\mathbf{r})\phi_B(\mathbf{r}) + - W_A(\mathbf{r})\phi_A(\mathbf{r}) - W_B(\mathbf{r})\phi_B(\mathbf{r}) + - \Psi(\mathbf{r})(1 - \phi_A(\mathbf{r}) - \phi_B(\mathbf{r}))\big] \quad (7)$$

Fields $\phi_A(\mathbf{r})$ and $\phi_B(\mathbf{r})$ are associated with normalized concentration profiles of A and B, and fields $W_A(\mathbf{r})$ and $W_B(\mathbf{r})$ with chemical potential fields acting on A and B, respectively; field $\Psi(\mathbf{r})$ enforces incompressibility. Evaluating functional integrals in Eq. 6 is a challenging task which, in principle, can be performed by field theoretic simulations as proposed and implemented by Fredrickson and coworkers [2, 11]. A simpler but approximate approach is based on the mean-field idea, where the dominant, and in fact only, contribution to the functional integral in Eq. 6 comes from the fields satisfying the saddle point condition expressed as the following set of equations:

$$\frac{\delta F}{\delta\phi_A} = \frac{\delta F}{\delta\phi_B} = \frac{\delta F}{\delta W_A} = \frac{\delta F}{\delta W_B} = \frac{\delta F}{\delta\Psi} = 0 \quad (8)$$

Performing the above functional derivatives yields

$$W_A(\mathbf{r}) = N\chi\phi_B(\mathbf{r}) + \Psi(\mathbf{r}) \quad (9)$$

$$W_B(\mathbf{r}) = N\chi\phi_A(\mathbf{r}) + \Psi(\mathbf{r}) \quad (10)$$

$$1 = \phi_A(\mathbf{r}) + \phi_B(\mathbf{r}) \quad (11)$$

$$\phi_A(\mathbf{r}) = \frac{V}{\mathcal{Q}}\int_0^f ds \, q(\mathbf{r}, s)q^\dagger(\mathbf{r}, s) \quad (12)$$

$$\phi_B(\mathbf{r}) = \frac{V}{\mathcal{Q}}\int_f^1 ds \, q(\mathbf{r}, s)q^\dagger(\mathbf{r}, s) \quad (13)$$

where $\mathcal{Q}/V$ can be calculated as

$$\frac{\mathcal{Q}}{V} = \frac{1}{V}\int d\mathbf{r}\; q(\mathbf{r},1)$$

and $q(\mathbf{r}, s)$ is the forward chain propagator which is the solution of the following modified diffusion equation

$$\begin{aligned} \frac{\partial q}{\partial s} &= \frac{1}{6}Na^2\nabla^2 q - W_A(\mathbf{r})q, \;\; 0 \le s \le f \\ \frac{\partial q}{\partial s} &= \frac{1}{6}Na^2\nabla^2 q - W_B(\mathbf{r})q, \;\; f \le s \le 1 \end{aligned} \tag{15}$$

with the initial condition $q(\mathbf{r}, 0) = 1$. Similarly $q^{\dagger}(\mathbf{r},s)$ is the backward chain propagator which is the solution of the conjugate modified diffusion equation:

$$\begin{aligned} -\frac{\partial q^{\dagger}}{\partial s} &= \frac{1}{6}Na^2\nabla^2 q^{\dagger} - W_A(\mathbf{r})q^{\dagger}, \;\; 0 \le s \le f \\ -\frac{\partial q^{\dagger}}{\partial s} &= \frac{1}{6}Na^2\nabla^2 q^{\dagger} - W_B(\mathbf{r})q^{\dagger}, \;\; f \le s \le 1 \end{aligned} \tag{16}$$

with the initial condition $q^{\dagger}(\mathbf{r},1) = 1$.

While the set of Eqs. 9, 10, 11, 12, and 13 can be solved, in principle, in a self-consistent manner, it is difficult to solve this set without some additional assumptions. Firstly, we assume that the melt forms a spatially ordered nanophase. Secondly, we use the UCA which is a considerable simplification, limiting our attention to a single D-dimensional spherical cell of radius R, and volume V. All fields, within this cell, have radial symmetry, which reduces this problem computationally to a single radial coordinate, r. The unconstrained spatial variables, specified in Table 1 for each d, become computationally irrelevant. Thus Eq. 14 can be rewritten as

$$\frac{\mathcal{Q}}{V} = D\frac{\int_0^R r^{D-1}q(r,1)dr}{R^D} \tag{17}$$

Note that the factor, D, in front of the above integral originates from the ratio of the area of a sphere with radius 1 to the volume of a spherical cell with the same radius, both in D dimensions.

While in integrals (Eqs. 12, 13 and 14) we replace $\mathbf{r}$ with r, and $d\mathbf{r}/V$ with $Dr^{D-1}dr/R^D$, in the modified diffusion Equations, 15 and 16, we replace $\mathbf{r}$ with r and use the spherically symmetric form of the Laplacian

$$\nabla^2 f = \frac{\partial^2 f}{\partial r^2} + \frac{D-1}{r}\frac{\partial f}{\partial r} \tag{18}$$

and similarly, in equations for both propagators $q(r, s)$ and $q^{\dagger}(r,s)$, we replace $\mathbf{r}$ with r. Obviously the solution depends on radius, R, and dimensionality, D = 1, 2, 3, 4 and 5, corresponding to 5 different nanophases, shown in Table 1. We use the Crank-Nicholson scheme [20] to solve iteratively the modified diffusion equations (Eqs. 15 and 16) in their radial form, until the self-consistency condition is met, obtaining the saddle point fields, $\overline{\phi_A}(r)$, $\overline{\phi_B}(r)$, $\overline{W_A}(r)$ and $\overline{W_B}(r)$ for a given R and D. In the MF approximation, the free energy functional becomes the free energy, and therefore we calculate the reduced free energy (per chain in k_BT units) by substituting the saddle point fields into Eq. 7:

$$\begin{aligned} \frac{F(R,D)}{nk_BT} \;\equiv\; -\ln\frac{\mathcal{Q}}{V} + \\ + \frac{D}{R^D}\int_0^R r^{D-1}\left[N\chi\overline{\phi_A}(r)\overline{\phi_B}(r) - \overline{W_A}(r)\overline{\phi_A}(r) - \overline{W_B}(r)\overline{\phi_B}(r)\right]dr \end{aligned} \tag{19}$$

III. RESULTS AND DISCUSSION

Since in the MF theory, the stability of a nanophase depends on the product χN and composition, f, we start at a given point of the phase diagram (f, χN) with a numerical calculation of $F(R, D)$ (Eq. 19) for various D's (1, 2, 3, 4, and 5) and R's. In order to solve the MDE's (Eqs. 15 and 16) we use up to N_T = 160 and up to N_R = 800 steps for the "time", s, and space, r, variables, respectively.

Numerically, we find R and D which minimize $F(R, D)$, and this allows us to determine the dimensionality, D, of the most stable nanophase, and therefore the most favorable nanophase itself, using the correspondence from Table 1. However, the free energy of this nanophase has to be compared to that of the disordered phase. Therefore, we calculate the difference

$$\frac{\Delta F}{nk_BT} \equiv \frac{F}{nk_BT} - \frac{F_{\mathrm{dis}}}{nk_BT} \tag{20}$$

where F_{dis} is the free energy of the disordered phase:

$$\frac{F_{\mathrm{dis}}}{nk_BT} = N\chi f(1-f) \tag{21}$$

If ΔF is negative then the appropriate nanophase is thermodynamically stable for the point considered, (f, χN); otherwise the system is the disordered phase. For example, in Figure 1 we compare $\Delta F/(nk_BT)$ for d = 4 and d = 5 as a function of f, at χN = 50. The intersection of those free energy curves occurs at f_{S_4/S_5} = 0.10418, as also indicated in Table 2.

This procedure allows us to map the DBC melt phase diagram for d = 5 in the (f, χN)-plane, as shown in Fig. 2. Since there is a mirror symmetry with respect to f = 0.5

($f \to 1-f$, A can be exchanged with B), we show the resultant nanophases only from $f = 0$ to 0.5, and the following phase sequence is observed: L, C, S_3, S_4, S_5 and the disordered phase; the corresponding data for those lines is presented in Table 2. A new nanophase, S_5, is observed in a relatively narrow strip between the S_4 phase and disordered phase.

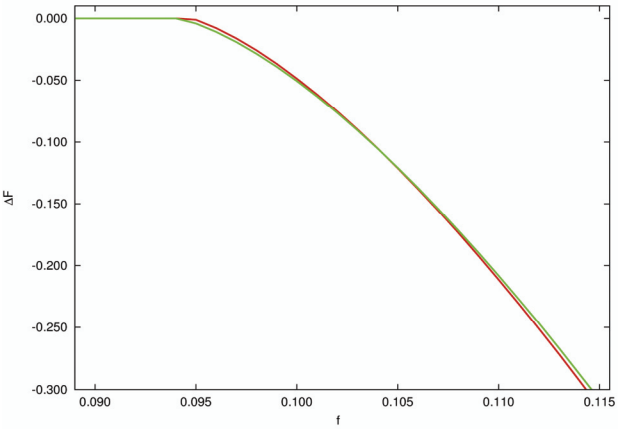

Fig. 1. χF (in nk_BT units) as a function of f for $\chi N = 50$. Red line indicates the results for the S_4 nanostructure and green line for the S_5 nanostructure. The lines intersect at $fS_4/S_5 = 0.10418$

Table 2. The ODT and OOT lines for selected χN's

χN	$f_{L/C}$	f_{C/S_3}	f_{S_3/S_4}	f_{S_4/S_5}	f_{ODT}
20	0.36797	0.25210	0.22436	0.21461	0.20541
30	0.34531	0.20048	0.16643	0.15475	0.14434
40	0.33601	0.17474	0.13631	0.12379	0.11347
50	0.33120	0.15988	0.11714	0.10418	0.09439
60	0.32828	0.15059	0.10379	0.09086	0.08086
70	0.32629	0.14452	0.09387	0.08043	0.07143
80	0.32482	0.14057	0.08698	0.07143	0.06383
90	0.32392	0.13737	0.08029	0.06556	0.05789
100	0.32303	0.13510	0.07535	0.05983	0.05332

This is the main result of this paper. We extrapolate the calculated OOT lines, $f_{L/C}, f_{C/S_3}, f_{S_3/S_4}, f_{S_4/S_5}$ to the strong segregation limit, that is, we estimate them as $\chi N \to \infty$ (or $1/(\chi N) \to 0$), fitting to the following function:

$$f(\chi N) = f^0 + \frac{g^0}{\chi N} \tag{22}$$

as used in referenced [9] and [20], where f^0 is the extrapolation to the strong segregation limit, and g^0 is a fitting parameter. The resultant limits, $f^0_{L/C}, f^0_{C/S_3}, f^0_{S_3/S_4}$, determined in Ref. 20 and $f^0_{S_4/S_5}$ (determined in this paper) are compared to the SST f's, as shown in Table 3. The discrepancy between the SST and the present SCFT with the UCA, for $f_{L/C}$ and f_{C/S_3} is within 2% error, as also reported in [9], and the discrepancy for f_{S_3/S_4} is about 10%. However, the difference between the extrapolated $f^0_{S_4/S_5} = 0.01$ and the calculated $f_{S_4/S_5} = 0.00018$ (from SST) is much larger. Since the SCFT is more advanced and accurate theory than the SST (the SCFT is a full mean field theory, and the SST is an approximation of the mean field theory which is meaningful only at strong segregations), we demonstrate that the area of stability for the S_5 phase is mostly likely to be significantly larger than that predicted from the SST.

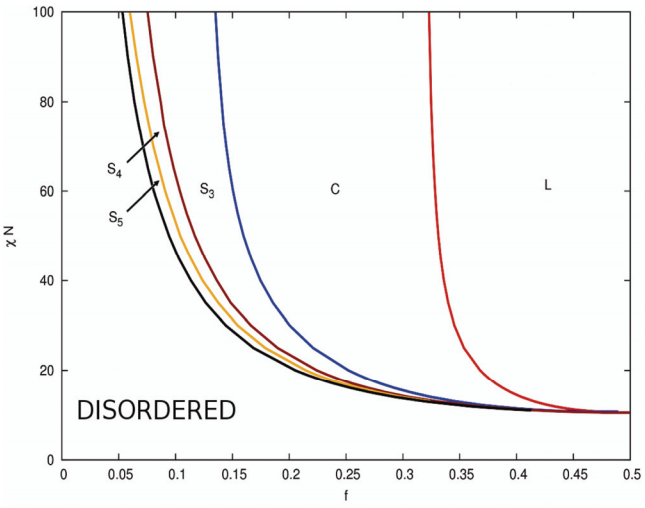

Fig. 2. DBC phase diagram in $5d$, L, C, S_3, S_4, and S_5 indicate corresponding nanophases; the disordered phase is also shown

Table 3. The OOT lines from the full SCFT [9] and UCA extrapolated to infinite χN's comparedto the SST results

Method	$f^0_{L/C}$	f^0_{C/S_3}	$f^0_{S_3/S_4}$	$f^0_{S_4/S_5}$
full SCFT	0.3100	0.1050	–	–
UCA	0.3150	0.1149	0.0306	0.010
SST	0.2999	0.1172	0.0336	0.00018

While spinodals for the ODT calculated with random-phase approximation (RPA) [5] are the same for $d = 2$, 3, 4 and 5, the binodals (the ODT lines), calculated in this work, depend on d as shown in Fig. 3. The binodals depend weakly on d, and they are particularly close to each other in the vicinity of $f_A = 1/2$ (symmetric diblock), and therefore

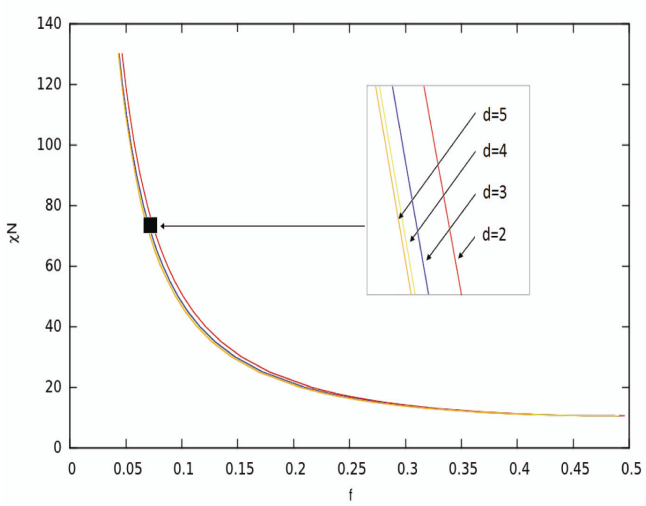

Fig. 3. The ODT lines for $d = 2$, 3, 4 and 5. The inset is from $\chi N = 70$ to 75

we show them in a narrow window (from 70 to 75 in χN, that is away from $f = 1/2$) in the inset of Fig. 3. We observe the sequence of binodals, as shown in the inset of Fig. 3. For $f = 1/2$ the RPA spinodal is at $(\chi N)_c \approx 10.4949$, and the calculated binodals (for $d = 2$, 3, 4 and 5) also converge to this point within the numerical accuracy. Similarly, the OOT lines seem to converge to $(\chi N)_c$ for $f = 0.5$.

IV. CONCLUSIONS

Using the self-consistent field theory in spherical unit cells of various dimensionalities, $D = 1$, 2, 3, 4 and 5, we calculate the phase diagram of a diblock, A-b-B, copolymer melt in 5-dimensional space, $d = 5$. The phase diagram is parameterized by the chain composition, f, and incompatibility between A and B, quantified by the product χN. We predict 5 stable nanophases: layers, cylinders, 3D spherical cells, 4D spherical cells and 5D spherical cells, and calculate both order-disorder and order-order transition lines. In the strong segregation limit, that is for large χN, the OOT compositions, $f_{L/C}$, f_{C/S_3}, f_{S_3/S_4} and f_{S_4/S_5} are determined by the strong segregation theory. While $f_{L/C}$, f_{C/S_3}, and f_{S_3/S_4} are close to the corresponding extrapolations from the self-consistent field theory, as shown in the previous study [20], the f_{S_4/S_5} extrapolation does not agree with the SST predictions. We find that the S_5 nanophase is stable in a narrow strip between ordered S_4 nanophase and the disordered phase. The calculated binodals (ODT lines) depend weakly on d, as expected.

Acknowledgments

We acknowledge a computational grant from the Poznan Supercomputing and Networking Center (PCSS).

References

[1] I.W. Hamley, Developments in Block Copolymer Science and Technology (John Wiley & Sons, Berlin, 2004).
[2] G.H. Fredrickson, The Equlibrium Theory of Inhomogeneous Polymers (Clarendon Press, Oxford, 2006).
[3] T.S. Bailey, C.M. Hardy, T.H. Epps, F.S. Bates, Macromolecules 35, 7007 (2002).
[4] M. Takenaka, T. Wakada, S. Akasaka, S. Nishisuji, K. Saijo, H. Shimizu, M.I. Kim, H. Hasegawa, Macromolecules 40, 4399 (2007).
[5] L. Leibler, Macromolecules 13, 1602 (1980).
[6] M. Banaszak, M.D. Whitmore, Macromolecules 25, 3406 (1992).
[7] J.D. Vavasour, M.D. Whitmore, Macromolecules 25, 5477 (1992).
[8] M.W. Matsen, M. Schick, Phys. Rev. Lett. 72, 2660 (1994).
[9] M.W. Matsen, M.D. Whitmore, J. Chem. Phys. 105, 9698 (1996).
[10] M.W. Matsen, J. Chem. Phys. 114, 10528 (2001).
[11] E.M. Lennon, K. Katsov, G.H. Fredrickson, Phys. Rev. Lett. 101, 138302 (2008).
[12] T. Taniguchi, Journal of the Physical Society of Japan 78, 041009 (2009).
[13] I.W. Hamley, Progress in Polymer Science 34, 1161 (2009).
[14] M.W. Matsen, in Soft Condensed Matter, Vol. 1, edited by G. Gompper and M. Schick (John Wiley & Sons, Berlin, 2005).
[15] E.W. Cochran, C.J. Garcia-Cervera, G.H. Fredrickson, Macromolecules 39, 2449 (2006).
[16] A.K. Khandpur, S. Forster, F.S. Bates, I.W. Hamley, A.J. Ryan, W. Bras, K. Almdal, K. Mortensen, Macromolecules 28, 8796 (1995).
[17] P.G. de Gennes, Scaling Concepts in Polymer Physics (Cornell University Press, Ithaca, 1979).
[18] M.W. Matsen, J. Phys.: Condens. Matter 14, R21 (2002).
[19] A.N. Semenov, Sov. Phys. JETP 61, 733 (1985).
[20] M. Banaszak, A. Koper, K. Lewandowski, P. Knychala, Submitted.

MICHAŁ DZIĘCIELSKI, received his MSc degree in Physics in 2011 from the Adam Mickiewicz University in Poznań where he is a PhD student in Physics. His research interests concern polymer physics, parallel algorithms, chemical reactions and programming.

KRZYSZTOF LEWANDOWSKI, received his MSc degree in Computer Science in 2007 from the Adam Mickiewicz University in Poznań where he is a PhD student in Physics. His research interests concern polymer physics, globular and micellar nanostructures, parallel algorithms and programming.

MICHAŁ BANASZAK, graduated in 1985 from Adam Mickiewicz University in Poznan, Poland. He received his PhD degree in Physics in 1991 from Memorial University in St. John's, Canada. From 1992 to 1995 he worked as postdoctoral fellow in Exxon Research & Engineering Co. in Annandale, New Jersey, USA, and from 1995 to 1997 in the Chemistry Department of UMIST in Manchester, UK. In 1997 he joined the Adam Mickiewicz University, obtaining the DSc degree (habilitation) in 2004 in Physics. His main interest is in developing new models and theories for nanoscale self-assembly of various copolymer systems.